

Received July 29, 2021, accepted September 3, 2021, date of publication September 10, 2021, date of current version September 27, 2021.

Digital Object Identifier 10.1109/ACCESS.2021.3111629

Vibration Characteristic Measurement Method of MEMS Gyroscopes in Vacuum, High and Low Temperature Environment and Verification of Excitation Method

WENHAO LUO^{1,2,3}, WEI SU^{1,2,3}, ZHENHUA NIE^{1,3}, QINWEN HUANG², SHIYUAN LI², AND XIANSHAN DONG²

¹MOE Key Laboratory of Disaster Forecast and Control in Engineering, Guangzhou 510632, China

²Science and Technology on Reliability Physics and Application Technology of Electronic Component Laboratory, China Electronic Product Reliability, and Environmental Testing Research Institute, Guangzhou 510610, China

³School of Mechanics and Construction Engineering, Jinan University, Guangzhou 510632, China

Corresponding authors: Wei Su (suwei@ceprei.com) and Zhenhua Nie (niezh@jnu.edu.cn)

This work was supported in part by the National Key Research and Development Program of China under Grant 2020YFB2008900, and in part by the Ministry of Education (MOE) Key Laboratory of Disaster Forecast and Control in Engineering, Jinan University, under Grant 20200904010.

ABSTRACT A method for measuring vibration characteristics of MEMS (Micro Electro Mechanical System) is presented. This method aims to simulate a real environment where MEMS operates. At first, the method of applying high and low temperature in a vacuum environment is studied. And the excitation method applying to movable microstructures of MEMS in this environment is found. Based on the above environmental conditions, the vibration characteristics of MEMS movable microstructure are measured by micro-laser vibration measurement. The base excitation method is used to measure the vibration characteristics of MEMS movable microstructures outside the plane. ANSYS 14.0 was used for finite element simulation to verify this method. The electrostatic excitation method is used to measure the inside of the plane. The stroboscopic method is used to verify the electrostatic excitation by fitting the displacement signal of the movable microstructure and the excitation output signal. The results show that the out-of-plane first-order frequency is 11.926 kHz, and the error is 0.30% compared with the experimental results. The amplitude is 44.218 nm, and the error is 0.59%. The in-plane first-order frequency is 5715.7Hz, which achieves the requirement of design precision. Both the numerical simulation and the stroboscopic method verify the excitation method well. The effect of temperature on the natural frequency of the structure is negatively correlated. And as the temperature drops, the motion of the structure becomes increasingly violent. The findings of this study provide important guidance for maintenance, reliable operation and optimal design of MEMS.

INDEX TERMS MEMS, reliability, vibration measurement with laser, vacuum, large temperature range.

I. INTRODUCTION

In recent decades, MEMS (Micro Electro Mechanical System) technology has achieved rapid development. MEMS Micro-Gyroscope has attracted more and more attention because of its small size and high precision [1], [2]. According to the different principles of micro gyroscope, it can be divided into Coriolis vibration gyroscope (CVG), fluid gyroscope, solid gyroscope, suspended rotor gyroscope, micro

The associate editor coordinating the review of this manuscript and approving it for publication was Michail Kiziroglou.

integrated optical gyroscope and atomic gyroscope. MEMS has broad development and market prospect in civil economic fields and national defense fields such as automobile navigation, mobile applications, aerospace and the foreseeable future high-tech battlefield. A well-known example is a marine gyrocompass developed by Sagem [3], [4]. As a member of the CVG family, the hemispherical resonator gyroscope (HRG) is small, easy to process, low-budget. And it does not require maintenance in long-term service [5]. These advantages allow it to be applied in the aerospace field [6].

However, MEMS may be subject to impact, high acceleration and large temperature range during service [7]. The movable microstructure in the device cannot operate stably. Some problems [8], [9] will lead to the failure of weapons and equipment, which seriously threaten the safe operation of spacecraft. Recently, some key space projects such as deep space exploration, manned spaceflight, and navigation satellites are continuously increasing. The reliability problem of devices under the vacuum and large temperature range environment is becoming more and more prominent, which needs to be solved urgently.

One way to improve the reliability is to take reliability parameters into account at the initial stage of device development. For example, some researchers theoretically studied the mechanical properties of nanostructured microbeams [10]–[11]. And other researchers analyzed the source of common defects in the manufacturing process of high-precision micro-shell resonators prepared by the micro-glass blowing process [12]–[15]. Another way is to conduct environmental experiments on the finished products and optimize them according to the test results. Recent reports document that temperature has a certain influence on the vibration characteristics of MEMS gyroscope, and the experimental verification was carried out. For example, Yunxiao Wu *et al.* found a positive correlation between temperature and natural frequency at standard atmospheric pressure [16]. Min Cui *et al.* designed a temperature compensation method to optimize the bias stability and angular rate walking parameters of MEMS gyroscopes [17]. Huiliang Cao *et al.* designed different methods to compensate for the temperature energy influence drift of the MEMS gyroscope [18]. Alireza Babaei investigated the relationship between optimized MEMS axial vibration frequency and taper parameters [19]. Xu Z analyzed the performance and accuracy of HRG with uneven electrostatic force caused by obvious an uneven capacitance gap [20]. However, aerospace devices often face vacuum, large temperature range and other conditions in service. The traditional contact measurement method is difficult to apply to millimeter-level components. It puts forward higher requirements for MEMS vibration characteristics measurement. Few researchers have addressed the problem of MEMS vibration characteristics measurement under these conditions.

This paper focuses on the failure of MEMS hermetically sealed devices in service. Operation environment simulation of devices is studied, including vacuum, high and low temperature environment application methods. The simulation results and stroboscopic photography are combined to verify the excitation method. It is found that the relationship between the natural frequency of the device and the temperature is negatively correlated, which is different from the findings in [16]. And the stroboscopic method is a very effective way to verify the excitation. The results provide useful guidance for the reliability optimization design of MEMS gyroscope.

II. DESIGN OF MESUREMENT TECHONLOGY SCHEME

The movable microstructure in MEMS has the characteristics of small size, small amplitude and high resonant frequency. According to the particularity of tests under high and low temperature environments, the conventional normal temperature test technology and method cannot completely satisfy the demands. Firstly, the excitation devices must be able to exert excitation on the movable microstructure under high and low temperature environments. Secondly, the methods must be nondestructive and non-contact for the test sample, and it can achieve nanoscale accuracy and high response of speed. Therefore, the exclusive measurement devices need to attach great importance in the following four aspects: method of applying vacuum and large temperature range, excitation method for microstructure, temperature control and vibration signal acquisition in this environment. Among them, the excitation way for microstructure and acquisition of vibration signal are the key points of vibration characteristic measurement.

III. METHOD OF APPLYING VACUUM, HIGH AND LOW TEMPERATURE ENVIRONMENT

A. METHOD OF APPLYING VACUUM ENVIRONMENT

In order to simulate the vacuum environment, the carrying platform is sealed in a cylindrical chamber with a diameter of 30cm. The chamber is equipped with two probe seats and two BNC lead interfaces for applying electrical signals to the movable microstructure and the base excitation device. The sealed chamber can be vacuumed by turbo-molecular pump to reach 0.01Pa, as shown in Fig. 1.

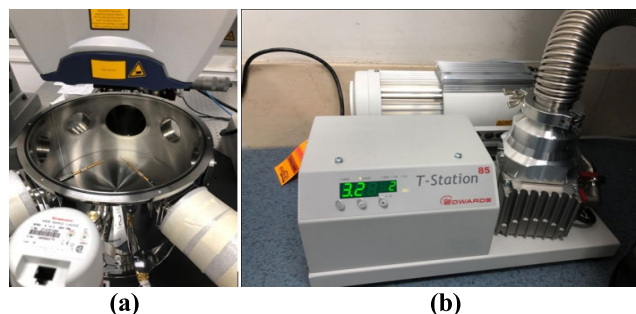


FIGURE 1. Devices of applying vacuum environment. (a)Vacuum chamber and (b)turbo-molecular pump developed by Janis, a American company.

B. METHOD OF APPLYING HIGH TEMPERATURE ENVIRONMENT

In order to measure the vibration of movable microstructure at high temperature, it is necessary to choose the appropriate heating method. Because electric heating can be automatic controlled with great precision, the sample is usually heated by electric heating in the laboratory. According to the power conversion mode, electric heating generally includes resistance heating, induction heating, arc heating, electron beam heating, dielectric heating and infrared heating, etc.

According to the influence of heating method on the environment, this study intends to choose electric resistance heating method. That is, the Joule heat generated by resistance is used to heat an object. There are two ways of electric resistance heating: One is that the heated object is heated directly through the current, which requires that the heated object is a conductor; the other is that the heated object is indirectly heated by heat transfer, and there is no special requirement for the type of heated object. In this experiment, the stage is heated and the samples are heated by heat transfer through the carrying platform.

C. METHOD OF APPLYING FRIGID TEMPERATURE ENVIRONMENT

There are two common ways to create a cold environment. One way is to set a semiconductor cold trap as refrigeration equipment. A water tank is arranged at the bottom of the cold trap for cooling the semiconductor refrigeration reactor in the cold trap to achieve $-50\text{ }^{\circ}\text{C}$ temperature environment. The other is to transport liquid nitrogen or liquid helium into the sealing chamber to cool the copper platform. The temperature can reach $-196\text{ }^{\circ}\text{C}$ by cooling with liquid nitrogen, while liquid helium can reach $-269\text{ }^{\circ}\text{C}$.

The effects of large temperature ranges on other equipment of the test are minimized as much as possible. The local heating or cooling method is used to heat or cool the platform through heat transfer. As shown in Fig. 2, a 50mm heating/cooling probe copper carrier is designed.

Because the faster cooling rate and higher temperature control accuracy should be obtained. For the movable microstructure, therefore, it is proposed to use the liquid nitrogen cooling method, transported by liquid nitrogen Dwar, as shown in Fig. 3, the target temperature is $-180\text{ }^{\circ}\text{C}$.

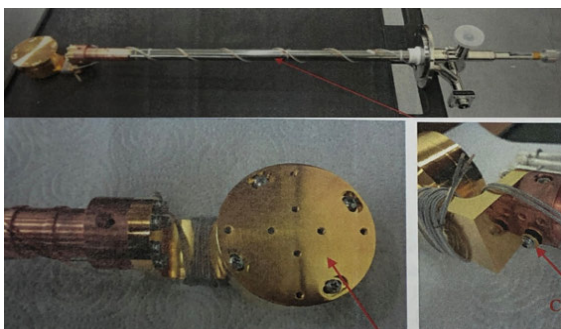


FIGURE 2. A 50mm heating/cooling probe copper platform developed by Janis, a American company.

D. METHOD OF TEMPERATURE CONTROL IN VACUUM ENVIRONMENT

Heating rod and 220V AC power supply are used, the highest temperature can reach $200\text{ }^{\circ}\text{C}$. Liquid nitrogen is used for cooling, and the lowest temperature can reach $-180\text{ }^{\circ}\text{C}$. The Lakeshore Model335 temperature controller is used, as shown in Fig. 4. The accuracy of temperature control can reach $0.05\text{ }^{\circ}\text{C}$, and the rise/drop rate is not controlled. They



FIGURE 3. LN-50 liquid nitrogen dewar developed by Janis, an American company.

all satisfy the temperature control demands of high and low temperature tests.

Temperature change in the vacuum can only be realized by thermal radiation or heat transfer, so the contact heat transfer device is adopted in this study. When the test is conducted at different temperatures, it must ensure that the temperature of the sample must be consistent with the platform. And adequate time to make the temperature stable must be allowed. It is also the key to ensure the accuracy of the measurement results.



FIGURE 4. Model 335 temperature controller.

In this study, the infrared thermal detector is used to measure the temperature of the samples and the carrying platform in real-time. The temperature stabilization time is obtained in two cases to ensure that the temperature of the sample reaches a predetermined value during the test. The two cases are as follows: (1)The sample is directly bonded to the carrier platform. (2)The sample is connected to the carrier platform through the piezoelectric ceramic base.

E. THE METHOD OF MAINTAINING VACUUM DURING GAS RELEASING IN HIGH TEMPERATURE

In the high-temperature environment, material gas release increases, resulting in a decrease of vacuum degree. It may not reach the limit of equipment at high temperatures. The method is to maintain a stable environmental condition in the process of the test when the vacuum degree has not reached the ultimate capacity of the equipment. The vacuum degree

of the above device belongs to open-loop control. When the device is turned on, the vacuum degree will continue to increase until it reaches the limit. When it is shut down, the vacuum degree will decrease slowly due to micro air leakage and material release. The vacuum can be controlled by a vacuum valve. After the vacuum degree reaches the predetermined value, the vacuum valve is properly reduced to make the release rate equal to the extraction rate. This process is measured and displayed by a pressure sensor, and it is manually controlled.

IV. CHOICE OF EXCITATION MODE

In the measurement process of microstructure vibration characteristics, the excitation method is crucial. An accurate frequency spectrum can be obtained by the proper excitation method. Otherwise, the interference frequency information may be introduced in the excitation process, resulting in inaccurate measurement results or false frequency.

This study attempts to use base excitation and electrostatic excitation. The electrostatic excitation method is to apply a sweeping signal to the movable microstructure to make it in operation mode. The vibration generated by this state is in-plane vibration. The piezoelectric ceramic with high-temperature resistance is used in the base excitation method. The sample is fixed on the excitation base, and the vibration of the base is used to drive the movable microstructure to generate forced vibration. This method enables the movable microstructure to generate out-of-plane vibration.

A. STUDY ON ELECTROSTATIC EXCITATION METHOD

According to the operation characteristics of the movable microstructures, the electrostatic excitation method is to apply DC+AC electrical signals to the structures. DC is the preset bias voltage and AC signal is the low voltage sweep signal. The vibration responses under three working conditions of high temperature, low temperature and normal temperature are measured by micro-laser vibrometer.

B. STUDY ON BASE EXCITATION METHOD

Considering the nonlinear coupled vibration effect caused by electrostatic excitation, the test results of microstructure frequency are affected. Therefore the base excitation method is used in this case. The sample is fixed on the piezoelectric ceramic base, and the movable microstructure is excited by the vibration of that base.

In the vacuum environment, the movable microstructure, piezoelectric ceramic and carrying platform must be connected together so that the temperature can be changed by thermal conduction. However, due to the high stiffness of the platform, the excitation characteristics of the piezoelectric ceramic will change after the connection. Meanwhile, the excitation signal input to the movable microstructure changes, which is likely to produce the information interference frequency. Consequently, the excitation features of the piezoelectric ceramic bonded to the platform are necessarily be studied.

To start with, the output vibration signal of the piezoelectric ceramic is measured, and its frequency response characteristics are analyzed. If there is interference frequency information, the simulation technology should be used to improve the connection between the base and the carrying platform. Simultaneously, the contact heat transfer should also be taken into account. The structure is similar to that of the shaking table, and the edge of the metal contact with the carrying platform for heat transfer. A damping pad is added between the piezoelectric ceramics and the platform to reduce the impact between them. The design scheme is shown in Fig. 5.

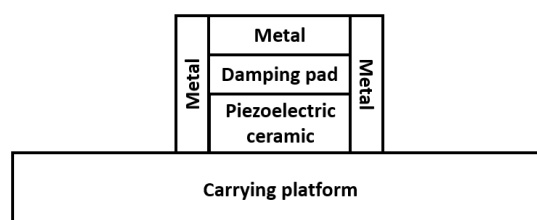


FIGURE 5. Design of piezoelectric ceramic base.

V. MEASUREMENT METHOD FOR VIBRATION SIGNALS OF MOVABLE MICROSTRUCTURES

Measurement methods can be roughly divided into two categories. One is the optical test method, which directly measures the motion of the structure. The laser doppler vibrometer is mainly used in this method. And the other is the electrical test method, which indirectly measures the motion of the structure.

A. OPTICAL TESTING METHOD

Movable microstructures can be evaluated at the wafer level. The test principle is as follows: The laser (wavelength λ) emitted by the sensor head hits the surface of the vibrating object, and then the laser is reflected soon. The reflection will produce frequency shift (Doppler f_D) due to the Doppler effect, and f_D is proportional to the object's speed v ($f_D = 2v/\lambda$), as is shown in Fig. 6. These signals are decoded so that the graph of time and velocity can be obtained. The current laser vibrometer can directly or indirectly obtain the velocity signal of the physical surface. The corresponding vibration signals of displacement or acceleration can be obtained by integration or differentiation.

1) MEASUREMENT OF IN-PLANE VIBRATION PARAMETERS OF MOVABLE MICROSTRUCTURE

In-plane vibration is the vibration of movable microstructure in the working plane. It is produced by the microstructure of the MEMS gyroscope during operation. The in-plane vibration measurement method is as follows: Firstly, the temperature and vacuum are adjusted to the predetermined conditions, and the electrostatic excitation method is adopted. DC+AC electric signal is applied to the actuating shaft to

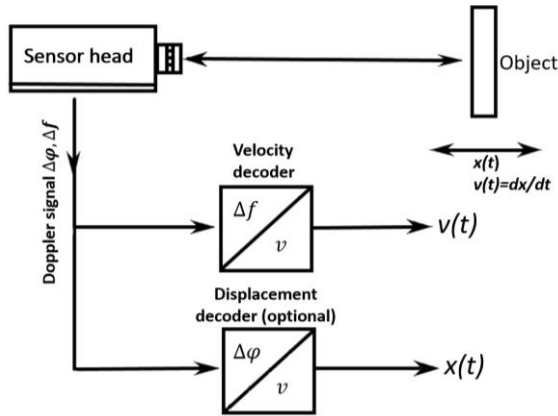


FIGURE 6. Test principle of scanning vibrometer.

make it vibrate in the working plane. The DC signal is a preset bias voltage, and the AC signal is a low-voltage sweep frequency signal. Afterward, the in-plane vibration response of movable microstructure is measured by micro-laser vibrometer. The in-plane vibration response characteristics are analyzed, and then the estimated values of these parameters are obtained. Finally, the in-plane vibration characteristic parameters are measured accurately by the stroboscope photograph method. The preset drive voltage DC value is adjusted and the parameters are repeatedly measured. The in-plane vibration characteristic parameters under various conditions are obtained.

2) MEASUREMENT OF OUT-OF-PLANE VIBRATION CHARACTERISTICS OF MOVABLE MICROSTRUCTURE

Out-of-plane vibration refers to the vibration of movable microstructure outside the working plane. It mainly comes from the unstable factors of the external environment. The method of out-of-plane vibration measurement is as follows: Firstly, the temperature and vacuum degree are also adjusted to a predetermined condition, and the piezoelectric ceramic base excitation method is adopted. The MEMS gyroscope is attached to the piezoelectric ceramic base, and a sinusoidal sweep signal is applied to the base to make the MEMS gyroscope microstructure vibrate out of the plane. Then, the out-of-plane vibration response is measured by micro-laser vibrometer, and the characteristic parameters of the out-of-plane vibration are obtained. Finally, the preset drive voltage DC value is adjusted and the parameters are repeatedly measured. The out-of-plane vibration characteristic parameters under various conditions are obtained.

B. ELECTRICAL TESTING METHOD

The principle of the frequency sweep test is based on the steady-state response of the inertial sensor. For MEMS gyroscopes packaged in high vacuum, the quality factor is often more than one hundred thousand or even millions. Therefore, it is difficult to obtain better results by adjusting parameters such as sweep number, sweep frequency bandwidth, interval

time and excitation signal size, and the test error is large and the time is longer. Therefore, this study intends to propose a nondestructive characterization of Q factor based on the vibration testing principle. Fig. 7 shows the test system block diagram. The system is mainly composed of LabVIEW software, NI PXI 4461 acquisition card, analog circuit and MEMS inertial sensor.

When the inertial sensor is stabilized by forced vibration, the response is a stationary solution. After the excitation signal is removed, the stationary solution of forced vibration will disappear. and the inertial sensor will turn into an underdamped vibration state, which is the transient response solution. Because the transient solution contains information such as resonant frequency and Q factor. Therefore, the resonant frequency and Q factor can be extracted by digital signal processing from the attenuation curve of underdamped vibration. The test steps are as follows: Firstly, the LabVIEW software applies the excitation signal $V_{ac} \sin(\omega t)$ to the inertial sensor through the acquisition card, so that the inertial sensor generates the steady-state response first. Then the excitation is stopped to get the inertial sensor into an underdamped vibration state. Finally, the transient response signal $x(t) = A_x e^{-\frac{\omega_d}{2Q_d} t} \sin\left(\sqrt{1 - \xi_d^2} \omega_d t + \cos^{-1} \xi_d\right)$ is collected into LabVIEW with an acquisition card for data analysis and processing. In LabVIEW software, wave peak detection technology, period average method and exponential fitting method can be used to quickly calculate the frequency and Q value. It realizes the new electrical nondestructive characterization of Q value.

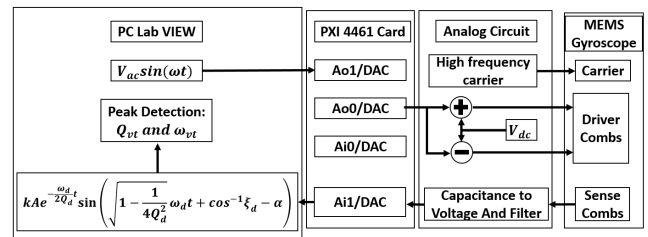


FIGURE 7. Q value of vibration test system principle block diagram.

1) CALCULATION OF QUALITY FACTOR

Quality factor Q can be used to characterize the change of vacuum degree. First of all, air leakage in the vacuum chamber or discharge of internal materials will lead to pressure changes. Second, temperature changes will lead to changes in internal gas Brownian motion, the internal pressure will also change. According to the fluid mechanics theory, Reynolds coefficient and damping coefficient will change with the pressure to affect the Q value. Therefore, the quality factor Q can be used to characterize the changes of temperature and pressure.

The resonant frequency is mainly affected by temperature because the temperature changes will change Young's modulus. Thus, the stiffness of the structure is affected and fatigue also causes degradation of the resonant frequency.

The resonance amplitude is proportional to the Q value, and the larger the Q value, the greater the amplitude. The resonant phase is generally -90° , mainly affected by the detection circuit filter or phase shifter.

The relationship between Q value and air pressure is as follows: The relationship between Q value and pressure is derived from the dynamic equation, thermodynamic equation and fluid dynamics equation of MEMS inertial sensor. The dynamic equation of the MEMS inertial sensor is

$$m_d \ddot{x}(t) + c_d \dot{x}(t) + k_d x(t) = F_0 \sin(\omega t) \quad (1)$$

Therefore, the relationship between Q value and damping coefficient can be expressed as:

$$Q_d = \frac{m_d \omega_d}{c_d} \quad (2)$$

According to the theory of fluid mechanics and gas viscosity, the Guet flow and Stokes flow model are used for the gyro with sliding film damping. The damping force coefficient is expressed as follows:

$$c_d = \frac{\mu A}{d} \quad (3)$$

where μ is the air viscosity coefficient, expressed as:

$$\mu = 0.3505 \rho \bar{v} \bar{\lambda} = 0.3505 n \bar{v} \bar{l} / V \quad (4)$$

According to thermodynamic theory and Boltzmann statistics, the average free path is mainly determined by temperature:

$$\bar{v} = \sqrt{\frac{3kT}{m}} \quad (5)$$

And the ideal gas state equation can be written as:

$$P = \frac{nkT}{V} \quad (6)$$

Therefore, the functional relationship between Q value and pressure P and gas number n can be induced by combining the above theories and equations. Thus, the degradation model of process parameter Q value can be obtained.

VI. VIBRATION CHARACTERISTIC MEASUREMENT OF MEMS

This study attempts to set up a vibration signal measurement platform for the optical testing method applying to movable microstructure. The movable microstructure can be measured in vacuum, high and low temperature environment without contact. The spectrum analysis of vibration signal is carried out by using the supporting software, and the modal parameters such as mode shape and natural frequency can be extracted by LMS Test.Lab modal analysis software.

According to the above scheme, the vibration characteristics measurement system is built, as shown in Fig. 8. It mainly includes the excitation device, measurement and analysis unit, temperature control unit and pressure control unit.

The sample which contained a comb structure for this test was a MEMS gyroscope of PMSC-7740, as shown in Fig. 9.

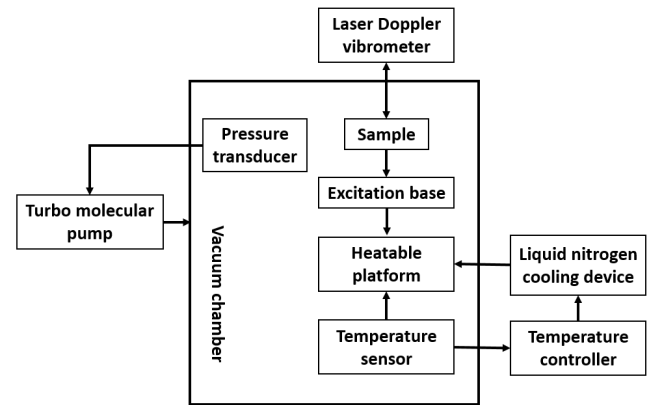


FIGURE 8. Block diagram of vibration characteristic measurement system of movable microstructures in vacuum environment of high and low temperature.

The working area mainly includes mass block, comb structure (capacitance) and micro-beam. This MEMS gyroscope can measure the dynamic parameters in two directions, as shown in Fig. 9(d). The mass blocks can move in x and y directions under external force. Then, the change of capacitance can generate a current signal for signal processing and unit sampling. Two of them were used in this experiment. Sample No. 2 was tested by the electrostatic excitation method, while sample No. 3 was tested by the base excitation method.

A. SIMULATION OF BASE EXCITATION METHOD

1) PROFILE MEASUREMENT OF MEMS

The MEMS movable microstructure measured by a surface profile measuring instrument was shown in Fig. 10(a). According to the height measurement, MEMS was a rectangular structure with a length of $5576.26 \mu\text{m}$ and a width of $4823.75 \mu\text{m}$. The MEMS was arranged on the base (including the shell, adhesive, chip and external lead), and the base was modeled in 3D. The simplified CAD model was shown in Fig. 10(b).

2) MATERIAL PROPERTY

ANSYS workbench [21] is used for this numerical simulation. The working area of the device included shell, adhesive, chip and external leads, etc. According to the literature review and relevant information of the sample, the material parameters set in the numerical simulation were shown in Table 1.

3) FINITE ELEMENT MODEL(FEM)

In this paper, according to the structure of MEMS, the modal analysis of MEMS was only calculated when the full constraints around MEMS, so the FEM was to establish the whole model of MEMS.

Before formal computation, grid independence verification was required to balance the computational accuracy with computational resource consumption. As shown in Fig. 11, 7 grids with different densities were used for modal analysis to extract the first-order frequencies of MEMS. When the

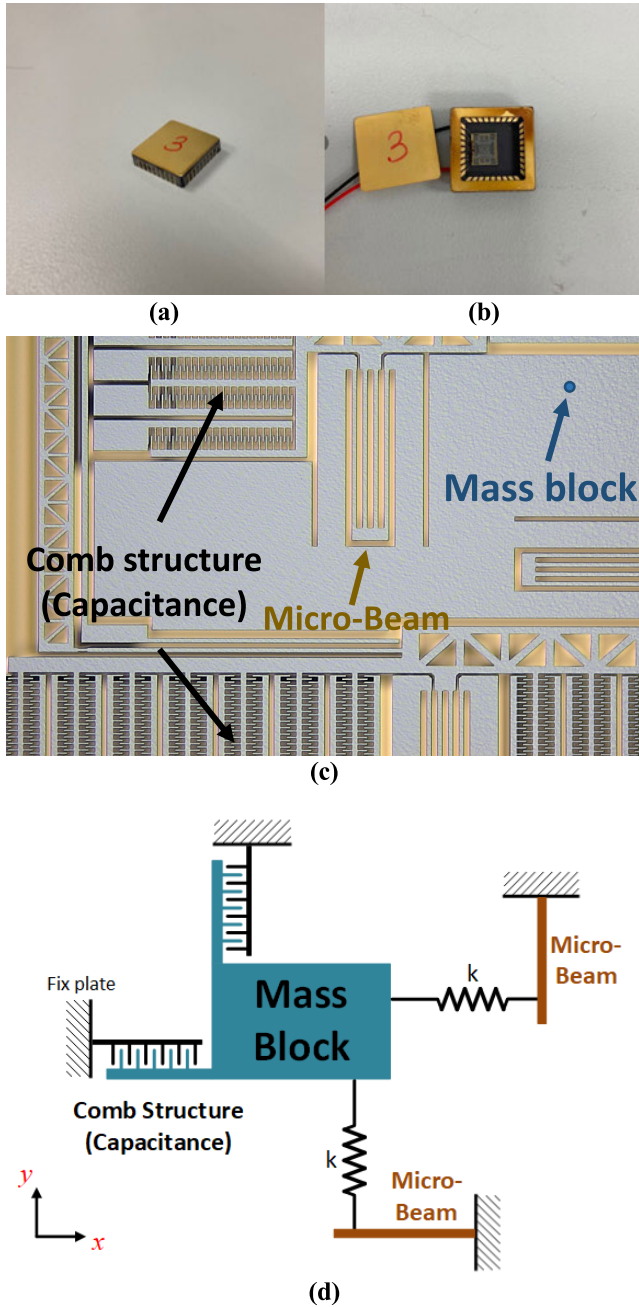


FIGURE 9. PMSC-7740 MEMS gyroscope. (a)Sealed sample, (b)Unsealed sample, (c) Five times magnification of comb structures, (d) Simplified mechanical structure schematic in the part of working area.

number of nodes was greater than 60000, the first-order natural frequency tends to be stable. Considering the calculation accuracy and the balance of computing resource consumption, a grid with 68524 nodes was used for calculation. In this model, the mesh was divided by sweeping mesh to generate hexahedral elements, as was shown in Fig. 12.

4) MODAL ANALYSIS

Full constraints were applied on the four ends of MEMS to solve their modes and extracted the first 10 natural

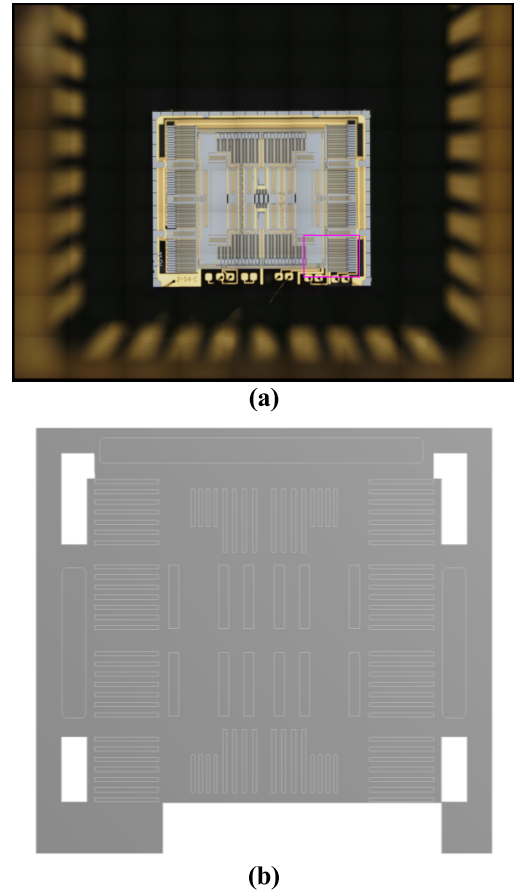


FIGURE 10. (a)MEMS measured by a surface profile measuring instrument, (b)Simplified CAD model of working area.

TABLE 1. Material properties.

density ρ (g/cm ³)	Elastic Modulus E (GPa)	Poisson ratio ν	Ultimate strength (GPa)	density ρ (g/cm ³)
lead	19.3	74.4	0.42	0.098~0.294
shell	3.9	400	0.22	0.2~0.3
adhesive	2	10	0.35	40~240
chip	2.3	190	0.28	7

frequencies, as shown in Table 2. The mode shapes at the first 2 natural frequencies were shown in Fig. 13. The view of the image was the isometric view. To make the shape obvious, the mode shape was enlarged.

5) HARMONIC RESPONSE ANALYSIS

When a linear structure is subjected to sinusoidal (harmonic) loads varying with time, its steady-state response can be determined by harmonic response. The structure will produce continuous periodic response after sustained periodic load [22]. From these curves, the “peak” response can be found and the stress corresponding to the peak frequency

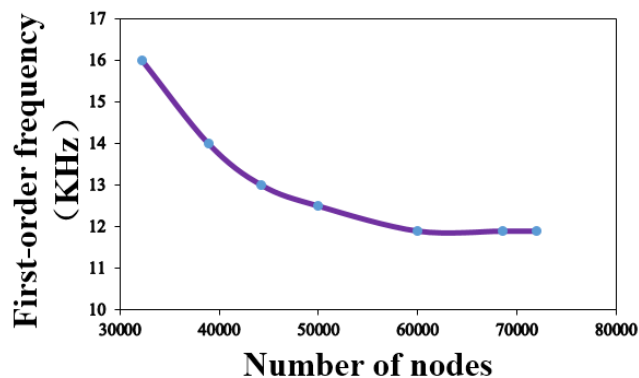


FIGURE 11. The relationship of the first-order frequency of MEMS and the number of nodes.

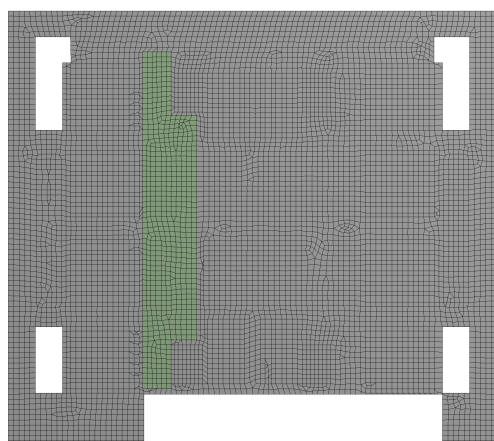


FIGURE 12. Mesh of FEM and observation area (marked in green).

TABLE 2. The first 10 natural frequencies.

Order	Natural Frequency (kHz)
1	11.89
2	25.69
3	91.61
4	103.07
5	166.71
6	213.97
7	283.13
8	346.43
9	400.60
10	505.27

can be observed. Harmonic response analysis only calculates the stable part of forced vibration but does not consider the transient vibration occurring at the beginning of excitation [23]. Harmonic response analysis enables designers to predict the long-term dynamic behavior of structures. This enabled the designer to verify that the design can successfully overcome resonance, fatigue, and other harmful factors caused by forced vibrations [24].

First, the peripheral framework of MEMS was fully constrained. Afterward, the green area shown in Fig. 14 was the

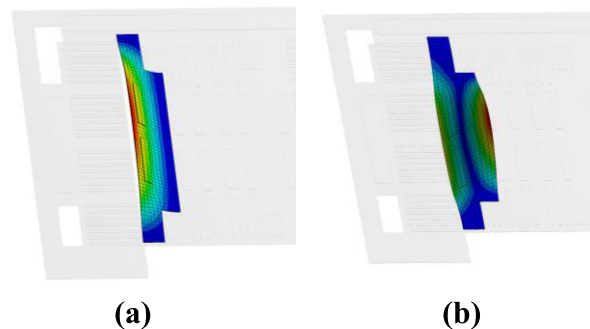


FIGURE 13. The mode shapes of the observed region of MEMS at different natural frequencies. (a) First-order Mode shape, (b) Second-order Mode shape.

area where the full constraint was applied. A sinusoidal force of 10N in the vertical direction was applied to the bottom of the shell. The frequency increased from 0kHz to 200kHz in increments of 1kHz. The displacement of the solder joint represented by the orange dot as shown in Fig. 14 was extracted, and it was applied to the FEM of MEMS to obtain the harmonic response of MEMS. Finally, the displacement of the highest point of the center of MEMS (displacement monitoring point, as shown in Fig. 14) is extracted to obtain the amplitude-frequency curve of MEMS under sinusoidal force excitation as shown in Fig. 15.

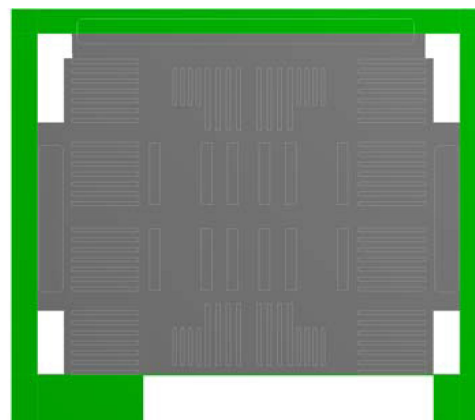


FIGURE 14. Figure of the MEMS constraint area and the position of the displacement monitoring point.

B. EXPERIMENT OF BASE EXCITATION METHOD

The base excitation method was to paste piezoelectric ceramic on the bottom of the sample, and its size was equivalent to the sample shell, as shown in Fig. 16. After processing the samples, sample No.3 was glued to the platform, and then the chamber was sealed and the air inside was pumped out to create a vacuum environment. The laser vibrometer was placed perpendicular to the surface of the sample along the direction of vibration, as shown in Fig. 17.

After the vacuum degree was reached, the laser vibrometer was started. The measuring points were arranged and the sampling parameters were set, as shown in Fig. 18. Subsequently,

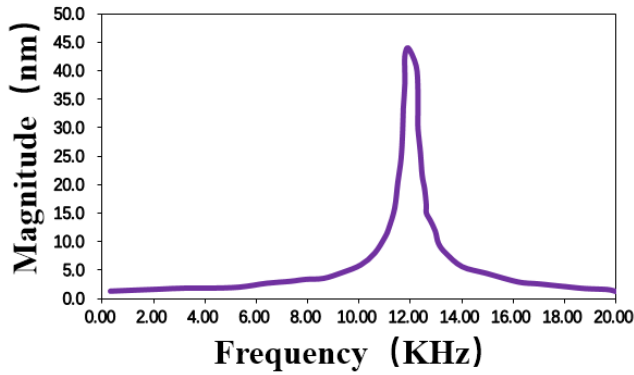


FIGURE 15. Amplitude-frequency curve of MEMS under sinusoidal force excitation.

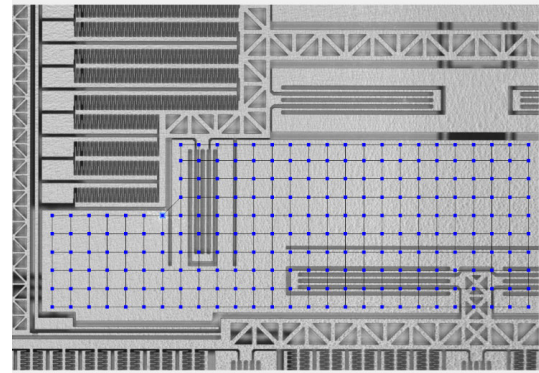


FIGURE 18. Measuring points were arranged on the mass plate.

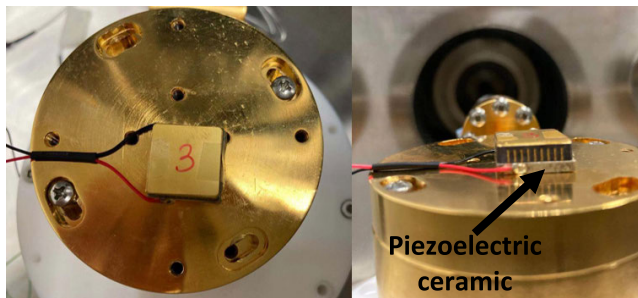


FIGURE 16. Piezoelectric ceramic was pasted on the bottom of the sample No.3.

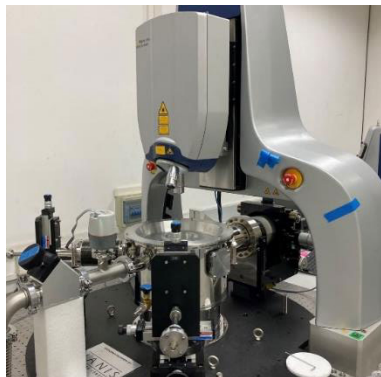


FIGURE 17. Micro-laser vibration measuring system. The laser vibrometer was developed by Polytec and the vacuum, devices of high and low temperature environment simulation was developed by Janis.

point was calculated by the PSV software in the laser vibration measuring system. The measured average spectrum and mode shape are shown in Fig. 20.

TABLE 3. Modal parameters.

Order	Natural Frequency (kHz)	Magnitude(nm)
1	11.926	44.218
2	25.702	8.4000

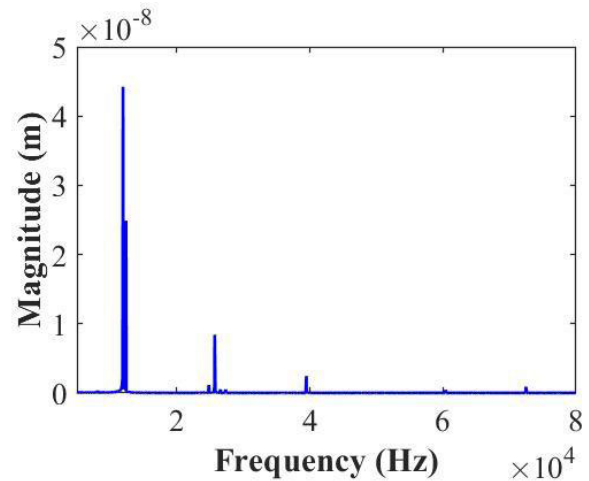


FIGURE 19. The displacement signals outside plane in frequency domain.

the piezoelectric ceramic was energized to vibrate and the laser source was used as the reference signal. Finally, the signal of each measuring point was sampled to calculate the frequency response function relative to the reference signal and response spectrum.

The bandwidth of the base excitation test was 312.5 kHz, the number of spectral lines was 409600, and the frequency resolution was 0.763Hz. As shown in Fig. 19 and Table 3, the modal parameters and the displacement signals in the frequency domain of each point were measured. The transfer function of each measuring point relative to the reference

C. ELECTROSTATIC EXCITATION TEST

According to the design of measurement in the previous chapter, the connection of electrostatic excitation mode was designed according to the actual operation of the sample. The detailed circuit of the sample was shown in Fig. 21. The carrier could make the structure move, while the drive shaft controlled the positive and negative movement of the structure in the X and Y direction. Because the carrier was too close to the driving positive to be welded, so the driving negative pole was chosen, as shown in Fig. 22.

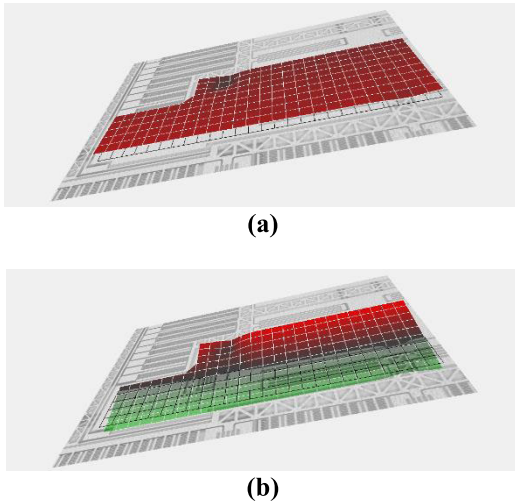


FIGURE 20. The first second order mode of the mass plate. (a)The first-order mode, (b)The second-order mode.

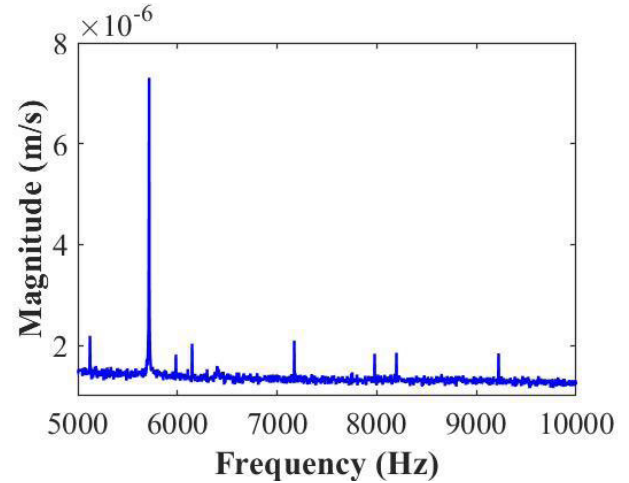


FIGURE 23. The in-plane vibration signals in frequency domain.

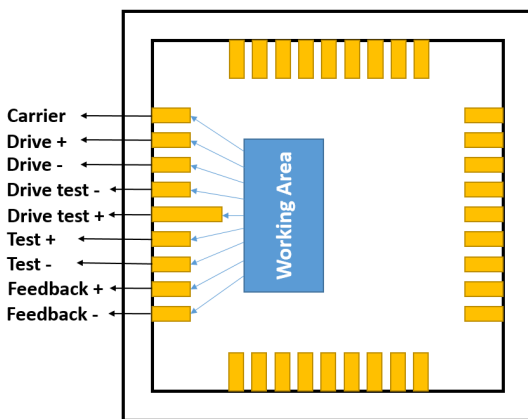


FIGURE 21. The detailed circuit of the sample.

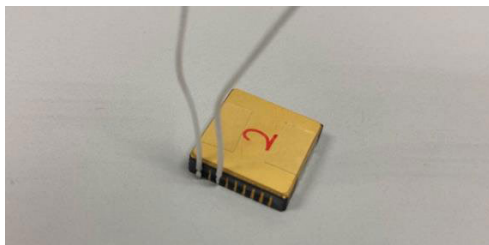


FIGURE 22. The carrier and the driving negative pole was chosen for a tin connection.

The experiment procedure was similar to the base excitation test. The difference is that the sample was directly electrified and the sinusoidal steady-state signal was input to measure the vibration parameters. The measured in-plane vibration of the structure is shown in Fig. 23.

1) EXPERIMENT IN HIGH AND LOW TEMPERATURE ENVIRONMENT

Based on the measurement in room temperature, additional conditions of large temperature variation are added. The

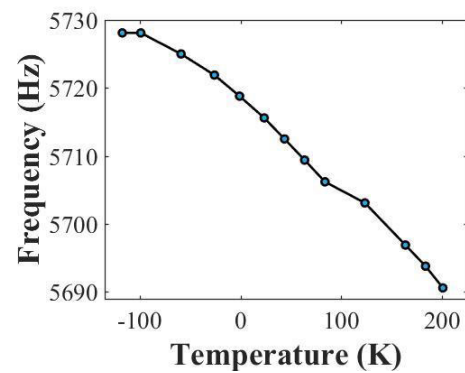


FIGURE 24. Frequency-temperature curve.

TABLE 4. The natural frequency changes at different temperatures.

Temperature(°C)	Natural Frequency of Mass Plate(Hz)
-117.55	5728.1
-99.15	5728.1
-59.15	5725.0
-26.05	5721.9
-1.08	5718.8
23.43	5715.6
43.58	5712.5
63.58	5709.4
83.75	5706.2
123.43	5703.1
163.66	5696.9
183.61	5693.8
200.85	5690.6

temperature ranged from 200°C to −117°C, and the natural frequency was recorded every time it changed. The results were shown in the following Table 4, and a frequency-temperature diagram is drawn, as shown in Fig. 24.

2) VERIFICATION OF ELECTROSTATIC EXCITATION METHOD
The peak frequency was 5715.7Hz according to Fig. 23. The movable microstructures moved most obviously at this

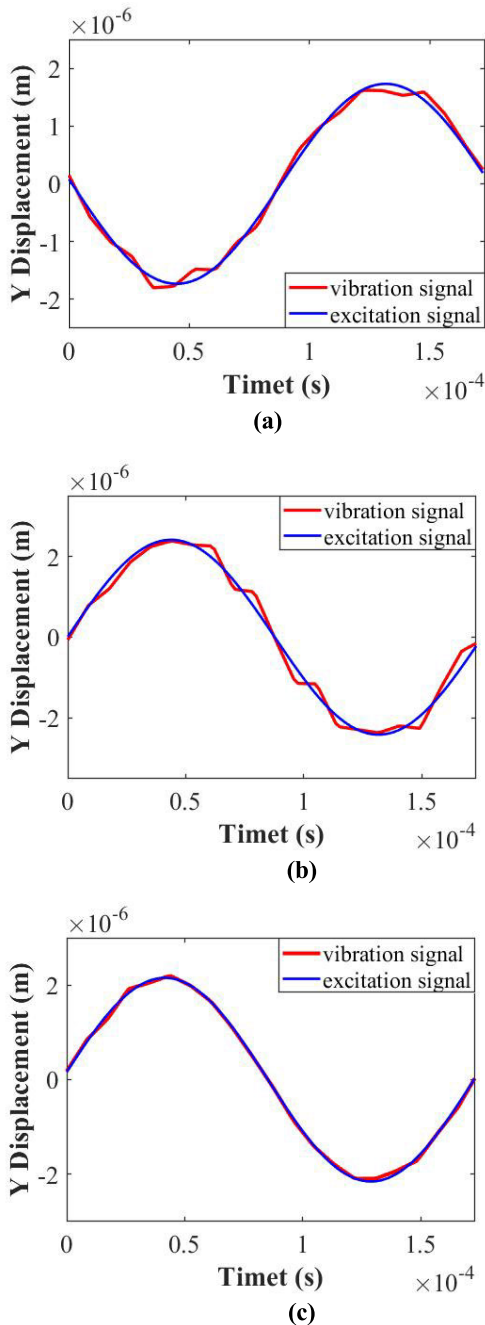


FIGURE 25. Displacement signal of the mass plate and excitation signal fitting. (a)room temperature, (b)200°C, (c) -115.15°C.

frequency. A sinusoidal excitation signal with a frequency of 5715.7Hz and a voltage of 5V was applied to obtain the displacement diagram of the movable microstructure during a motion period by the stroboscope photograph method. Finally, the displacement diagram was fitted with the input sinusoidal signal, and the electrostatic excitation method was verified by comparing the deviation, as shown in Fig. 25.

3) COOLING CHARACTERISTIC

When the temperature continuously dropped from the normal temperature, the mass plate vibrates at a high

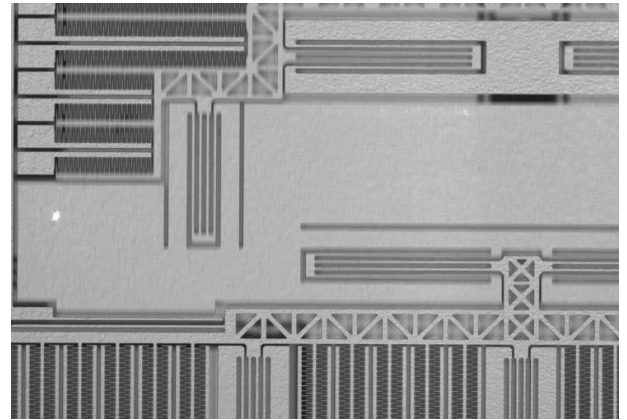


FIGURE 26. The vibration position imaging is blurred while the non-vibration position is clear.

frequency after continuously energizing for about 30min. The criterion is that the vibration position imaging is blurred and the non-vibration position is clear, as shown in Fig. 26.

VII. CONCLUSION

A method for measuring vibration characteristics of MEMS devices is designed. The application of vacuum, high and low temperature environment is studied, and a suitable measuring system is built. Two excitation schemes are designed to measure the natural frequencies of the movable microstructures. The vibration characteristic parameters outside the plane at room temperature are measured by the base excitation method and verified by the ANSYS numerical simulation results. The electrostatic excitation method is used to measure the parameters under common, high and low temperature, and the stroboscope photograph method is used to verify this method.

The results show that when the base excitation mode is used, the simulation result of the first-order natural frequency is 11.89kHz. And the error between the experimental results and the simulation is 0.30%. The simulation result of displacement amplitude is 43.96nm, and the error between the experimental value and the simulation value is 0.59%. These results prove the feasibility of the base excitation method. The electrostatic excitation method compares vibration signal with input sinusoidal steady-state excitation signal. As shown in Fig. 26, they are well fitted and the excitation method is also well verified. Moreover, the temperature is negatively correlated with the natural frequency of the structure. The motion of movable microstructures becomes more and more intense when the temperature is continuously dropped below room temperature. Due to the severe vibration, the movable microstructure performs periodic motion more stable, so the sine fitting effect is the best. Surprisingly, the sample did not fail in the temperature range tested in this experiment. Finally, the natural frequency of in-plane vibration is less than that of out-of-plane vibration, which is important guidance to improve the reliability of MEMS. The test system well simulates the harsh environment where the device operates.

Compared with the contact vibration measurement, the non-contact method is not affected by the mass of the strain gage and the relative size of the viscous strain gage and the sample to be measured. The response speed of this system is high, and the accuracy of measuring displacement achieves nanoscale displacement.

REFERENCES

- [1] K. Liu, W. Zhang, W. Chen, K. Li, F. Dai, F. Cui, X. Wu, G. Ma, and Q. Xiao, "The development of micro-gyroscope technology," *J. Micromech. Microeng.*, vol. 19, no. 11, pp. 113001–113029, 2009.
- [2] N. Yazdi, F. Ayazi, and K. Najafi, "Micromachined inertial sensors," *Proc. IEEE*, vol. 86, no. 8, pp. 1640–1659, Aug. 1998.
- [3] A. Jeanroy, G. Grosset, J.-C. Goudon, and F. Delhaye, "HRG by Sagem from laboratory to mass production," in *Proc. IEEE Int. Symp. Inertial Sensors Syst.*, Feb. 2016, pp. 1–4.
- [4] A. Jeanroy, A. Bouvet, and G. Remillieux, "HRG and marine applications," *Gyroscopy Navigat.*, vol. 5, no. 2, pp. 67–74, Apr. 2014.
- [5] A. D. Matthews and D. A. Bauer, "Hemispherical resonator gyro for precision pointing applications," *Proc. SPIE*, vol. 2466, pp. 128–139, Jun. 1995.
- [6] C. Negri, E. Labarre, C. Lignon, E. Brunstein, and E. Salaün, "A new generation of IRS with innovative architecture based on HRG for satellite launch vehicles," *Gyroscopy Navigat.*, vol. 7, no. 3, pp. 223–230, Jul. 2016.
- [7] D. M. Tanner, J. A. Walraven, K. S. Helgesen, L. W. Irwin, D. L. Gregory, J. R. Stake, and N. F. Smith, "MEMS reliability in a vibration environment," in *Proc. 38th Annu. IEEE Int. Rel. Phys. Symp.*, Apr. 2000, pp. 139–145.
- [8] M. L. Hoang and A. Pietrosanto, "A new technique on vibration optimization of industrial inclinometer for MEMS accelerometer without sensor fusion," *IEEE Access*, vol. 9, pp. 20295–20304, 2021.
- [9] J. Liu, Y. Yang, S. Guo, B. Fan, L. Xuan, F. Bu, and D. Xu, "A novel compensation method for eliminating precession angular-rate bias in MEMS rate-integrating gyroscopes," *IEEE Access*, vol. 8, pp. 145611–145619, 2020.
- [10] M. H. Jalaei and Ö. Civalek, "On dynamic instability of magnetically embedded viscoelastic porous FG nanobeam," *Int. J. Eng. Sci.*, vol. 143, pp. 14–32, Oct. 2019.
- [11] Ç. Demir and Ö. Civalek, "On the analysis of microbeams," *Int. J. Eng. Sci.*, vol. 121, pp. 14–33, Dec. 2017.
- [12] M. H. Asadian and A. M. Shkel, "Fused quartz dual shell resonator," in *Proc. IEEE Int. Symp. Inertial Sensors Syst. (INERTIAL)*, Apr. 2019, pp. 1–4.
- [13] I. P. Prikhodko, S. A. Zotov, A. A. Trusov, and A. M. Shkel, "Microscale glass-blown three-dimensional spherical shell resonators," *J. Micromech. Syst.*, vol. 20, no. 3, pp. 691–701, 2011.
- [14] J. Y. Cho and K. Najafi, "A high- q all-fused silica solid-stem wineglass hemispherical resonator formed using micro blow torching and welding," in *Proc. 28th IEEE Int. Conf. Micro Electro Mech. Syst. (MEMS)*, Jan. 2015, pp. 821–824.
- [15] M. J. Ahamed, D. Senkal, and A. M. Shkel, "Effect of annealing on mechanical quality factor of fused quartz hemispherical resonator," in *Proc. Int. Symp. Inertial Sensors Syst. (SISS)*, Feb. 2014, pp. 1–4.
- [16] Y. Wu, Y. Pan, D. Wang, T. Qu, and Y. Huang, "The study on temperature characteristics of a monolithic fused silica cylindrical resonator," in *Proc. Joint Int. Inf. Technol., Mech. Electron. Eng.* Amsterdam, The Netherlands: Atlantis Press, 2016, pp. 44–49.
- [17] M. Cui, Y. Huang, W. Wang, and H. Cao, "MEMS gyroscope temperature compensation based on drive mode vibration characteristic control," *Micromachines*, vol. 10, no. 4, p. 248, Apr. 2019.
- [18] H. Cao, Y. Zhang, C. Shen, Y. Liu, and X. Wang, "Temperature energy influence compensation for MEMS vibration gyroscope based on RBF NN-GA-KF method," *Shock Vib.*, vol. 2018, pp. 1–10, Dec. 2018.
- [19] A. Babaei, "Longitudinal vibration responses of axially functionally graded optimized MEMS gyroscope using Rayleigh–Ritz method, determination of discernible patterns and chaotic regimes," *Social Netw. Appl. Sci.*, vol. 1, no. 8, pp. 1–12, Aug. 2019.
- [20] Z. Xu, G. Yi, M. Er, and C. Huang, "Effect of uneven electrostatic forces on the dynamic characteristics of capacitive hemispherical resonator gyroscopes," *Sensors*, vol. 19, no. 6, p. 1291, Mar. 2019.
- [21] *ANSYS Fluent Theory Guide, Release 14.0*, ANSYS, Canonsburg, PA, USA, Nov. 2011.
- [22] Y. Peng, H. Zhao, F. Bu, L. Yu, D. Xu, and S. Guo, "An automatically mode-matched MEMS gyroscope based on phase characteristics," in *Proc. IEEE 3rd Inf. Technol., Netw., Electron. Autom. Control Conf. (ITNEC)*, Mar. 2019, pp. 2466–2470.
- [23] Y. Luo, Y. Pan, Z. Qiu, Z. Fan, G. Xiao, X. Yu, H. Luo, and S. Asokanathan, "Observation and prediction for frequency split of cylindrical resonator gyroscopes subject to varying angular velocity," in *Proc. IEEE Int. Symp. Inertial Sensors Syst. (INERTIAL)*, Mar. 2020, pp. 1–4.
- [24] W. Zhao, H. Yang, L. Song, X. Yu, F. Liu, and Y. Su, "Researched on the bias stability of the HRG affected by the temperature and the standing wave azimuth," *Meas. Control*, vol. 53, nos. 9–10, pp. 1730–1738, Nov. 2020.

• • •